Properties of Gd2O3 nanoparticles studied by hyperfine interactions and magnetization measurements

E. L. Correa, B. Bosch-Santos, F. H. M. Cavalcante, B. S. Correa, R. S. Freitas, A. W. Carbonari, and M. P. A. Potiens

Citation: AIP Advances **6**, 056112 (2016); doi: 10.1063/1.4943601
View online: http://dx.doi.org/10.1063/1.4943601
View Table of Contents: http://scitation.aip.org/content/aip/journal/adva/6/5?ver=pdfcov
Published by the AIP Publishing

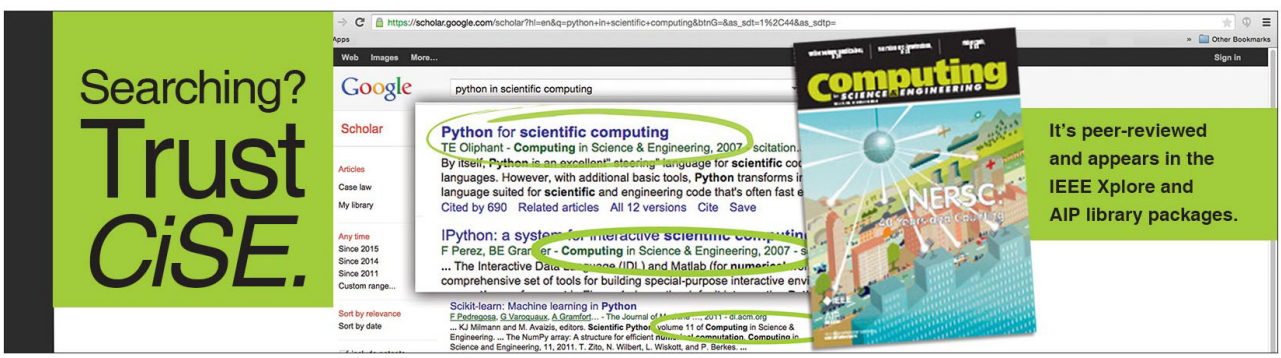

Properties of Gd_2O_3 nanoparticles studied by hyperfine interactions and magnetization measurements

E. L. Correa,[1,a] B. Bosch-Santos,[1] F. H. M. Cavalcante,[1] B. S. Correa,[2] R. S. Freitas,[3] A. W. Carbonari,[1] and M. P. A. Potiens[1]
[1]*Instituto de Pesquisas Energéticas e Nucleares, University of São Paulo, 05508-000, São Paulo, Brazil*
[2]*Faculdade de Ciências Exatas e Tecnologia, Federal University of Pará, 68440-000, Abaetetuba, PA, Brazil*
[3]*Instituto de Física, University of São Paulo, CP 66318, 05314-970, São Paulo, SP, Brazil*

(Presented 12 January 2016; received 6 November 2015; accepted 22 December 2015; published online 4 March 2016)

The magnetic behavior of Gd_2O_3 nanoparticles, produced by thermal decomposition method and subsequently annealed at different temperatures, was investigated by magnetization measurements and, at an atomic level, by perturbed $\gamma - \gamma$ angular correlation (PAC) spectroscopy measuring hyperfine interactions at ^{111}In(^{111}Cd) probe nuclei. Nanoparticle structure, size and shape were characterized by X-ray diffraction (XRD) and Transmission Electron Microscopy (TEM). Magnetization measurements were carried out to characterize the paramagnetic behavior of the samples. XRD results show that all samples crystallize in the cubic-C form of the bixbyite structure with space group *Ia*3. TEM images showed that particles annealed at 873 K present particles with highly homogeneous sizes in the range from 5 nm to 10 nm and those annealed at 1273 K show particles with quite different sizes from 5 nm to 100 nm, with a wide size distribution. PAC and magnetization results show that samples annealed at 873 and 1273 K are paramagnetic. Magnetization measurements show no indication of blocking temperatures for all samples down to 2 K and the presence of antiferromagnetic correlations. [http://dx.doi.org/10.1063/1.4943601]

I. INTRODUCTION

Nanotechnology is nowadays a fast growing field of study with huge potential for medical applications such as tumor detection and treatment.[1–5] As a promising material for these applications, gadolinium nanoparticles (GdNP) currently have been of great interest mainly because their paramagnetic and atomic properties. The high magnetic moment of Gd^{3+} ion, for instance, resulting in an intense magnetic interaction with external magnetic fields, enable GdNP to be used as magnetic resonance imaging (MRI) contrast agent.[6,7] Besides being developed for MRI contrast enhancement and multimodal imaging, GdNP also have been considered as a potential material in tumor therapy by thermal neutrons irradiation.[8] Therefore, it is important to have a good structural and magnetic characterization of this compound within an atomic scale.

In this paper, besides magnetization measurements, perturbed-angular-correlation (PAC) spectroscopy was used to measure hyperfine interactions in Gd_2O_3 nanoparticle samples. This powerful method allows, within an atomic range, the study of magnetic and structural phase transitions, oxidation reactions, and the defect chemistry in oxides.[9] Gd_2O_3 nanoparticles were produced by thermal decomposition method with the incorporation, during preparation, of radioactive ^{111}In(^{111}Cd) probe nuclei for PAC measurements. Thermal decomposition is considered a good method to produce nanoparticles for medical applications resulting in homogenous nanostructures

[a]Electronic mail: eduardo.correa@usp.br

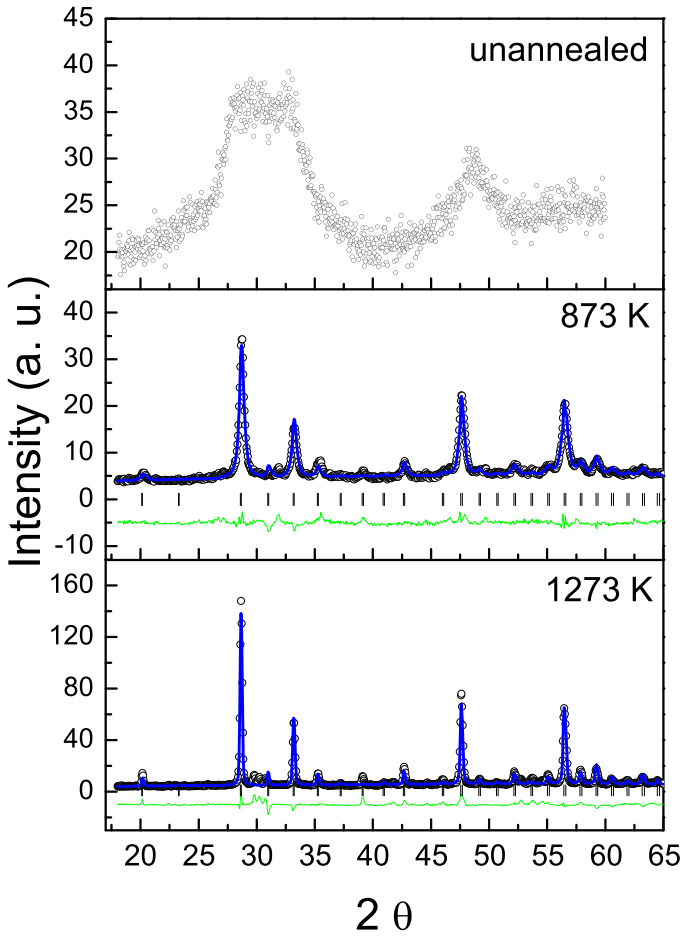

FIG. 1. X-ray diffraction patterns for Gd_2O_3 samples. Solid lines are the least squares fit of the Rietveld method to the experimental data.

with narrow size distribution.[10] Samples were characterized by transmission electron microscopy (TEM) and X-ray diffraction (XRD). Magnetization measurements were performed to characterize the paramagnetism of samples.

II. EXPERIMENTAL PROCEDURE

Gd_2O_3 nanoparticles were obtained by adding 2 mmol of $C_6H_9GdO_6$ into 20 mL of diphenyl ether with 4 mmol of oleylamine, 6 mmol of oleic acid and 10 mmol of 1,2-octanediol. Approximately 20-30 μCi of carrier-free ^{111}In(^{111}Cd) probe nuclei were added to the solution, which was stirred and heated for about 4 hours under O_2 atmosphere. After cooling to room temperature 20 mL of methanol were added to the solution, which was centrifuged for about two hours in order to precipitate the solid. Washing was performed in two steps using, first, 15 mL and, second, 10 mL of methanol. The resulting solid was dried under vacuum for 24 hours. The sample was then divided into three parts: one part was characterized as it (sample 1), the second part was annealed for 10 hours at 873 K (sample 2) and the third part was annealed for 10 hours at 1273 K (sample 3).

PAC spectroscopy was performed in a system with four BaF_2 detectors associated with a slow-fast setup used to measure delayed gamma-gamma coincidences. This technique consists in detecting two gamma radiations in a cascade as result of the decay from the excited levels of probe nuclei. The angular correlation of these gamma rays is perturbed by the interaction between the nuclear moment of the intermediate nuclear state and extra nuclear fields. A home developed software was used to process the coincidence spectra in order to obtain the perturbation function

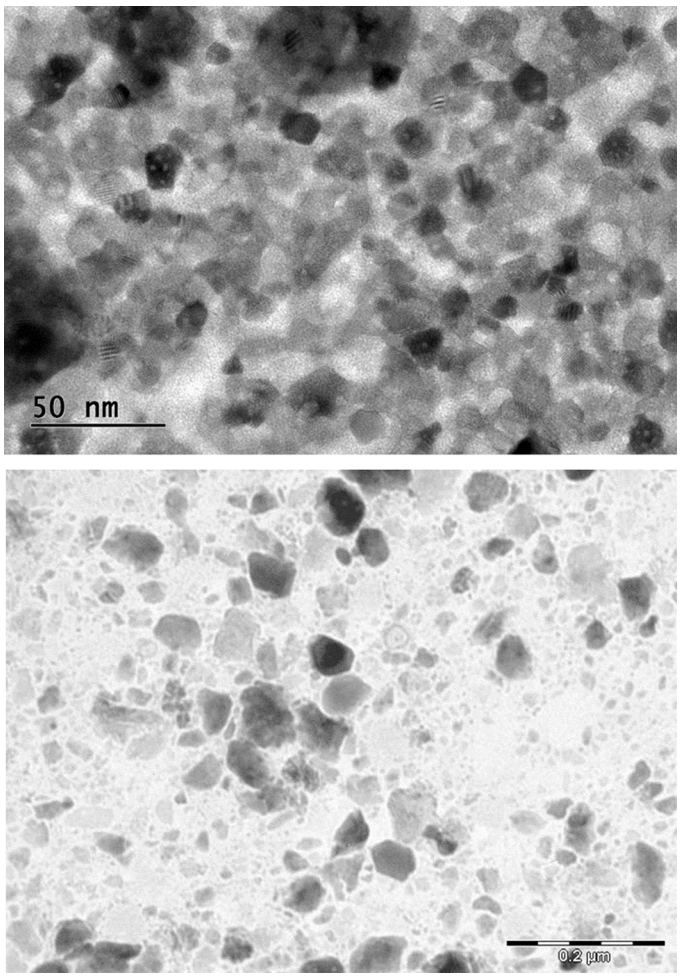

FIG. 2. Transmission electron microscopy images for Gd_2O_3 sample 2 (top) and sample 3 (bottom).

$R(t) = A_{22}G_{22}(t)$, where A_{22} is the anisotropy factor and G_{22} (t) is the perturbation function that takes into account the hyperfine interactions. G_{22} can be modeled in terms of theoretical functions accounting for magnetic dipole and/or electric quadrupole interactions. It provides detailed description of hyperfine interactions and allows the determination of the magnetic hyperfine field and electric field gradient. More information about PAC measurements can be found elsewhere.[11–13] PAC measurements were carried out at different temperatures: 77 K and 293 K, 473 K, 673 K, 873 K. Sample 3 was also measured at 1073 K.

After ^{111}In decay X-ray diffraction (XRD), Transmission Electron Microscopy (TEM) and magnetization were performed in both samples. TEM was used to characterize the material concerning the nanoparticles crystal structure, shape, size and size distribution. XRD results were analyzed by the Rietveld method. The magnetic measurements were carried out in a magnetometer with a superconducting quantum interference device (SQUID) sensor (MPMS-XL, Quantum Design).

III. RESULTS AND DISCUSSION

A. X-ray diffraction and transmission electron microscopy

Results for the X-ray diffraction (see Fig. 1) showed the expected Gd_2O_3 cubic structure, which belongs to the $Ia3$ space group, with lattice parameters of a=b=c=10.80481(2) Å for sample 2 and a=b=c=10.80591(3) Å for sample 3, which are quite close to a=b=c=10.82311(20) Å previously reported.[14] The diffraction pattern for sample 1 shows broad peaks indicating very small

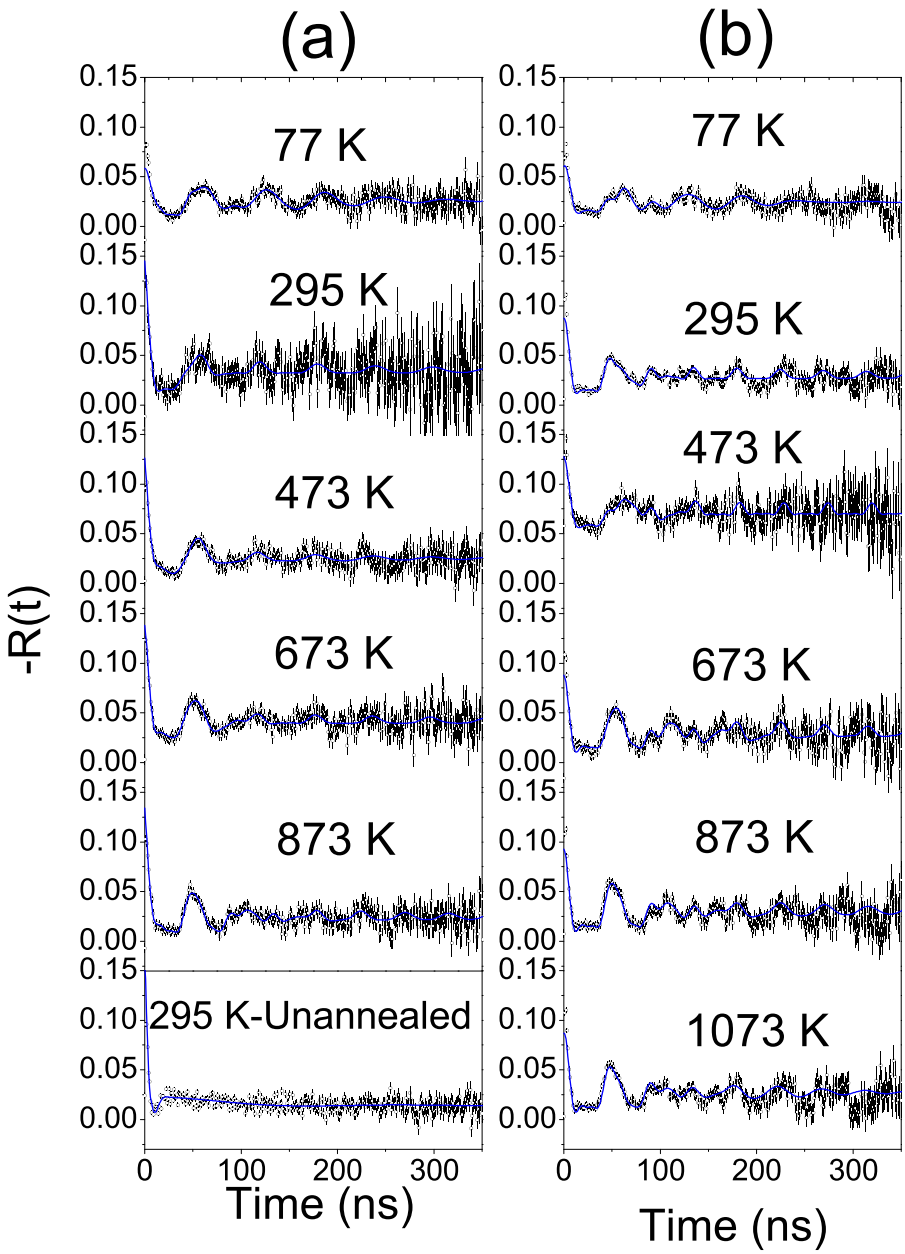

FIG. 3. Perturbation functions for (a) sample 2 and (b) sample 3 of Gd_2O_3 measured with ^{111}Cd probes at different temperatures. Result for sample 1 measured at room temperature is shown at the bottom of column a. Solid lines are the least squares fit of the theoretical functions to the experimental data.

nanoparticles. Transmission electron microscopy images are displayed in Fig. 2 and the results show particles with highly homogeneous sizes in the range from 5 nm to 10 nm for sample 2. Results for sample 3 show particles with quite different sizes from 5 nm to 100 nm indicating that the annealing at 1273 K resulted in particle clustering.

B. PAC measurements

PAC spectra obtained at different temperatures for samples 2 and 3 along with a spectrum measured at room temperature for sample 1 are shown in Fig. 3, where the solid lines are the best fit of the theoretical functions to the experimental data.

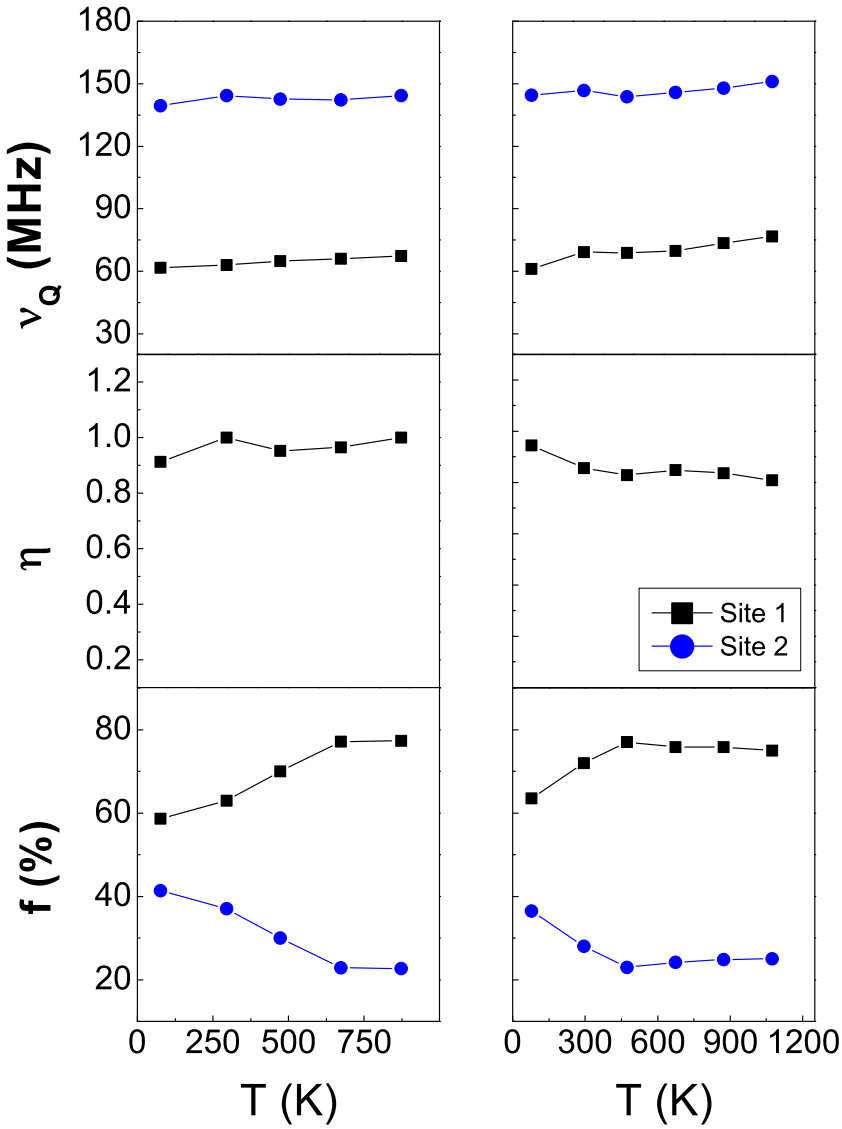

FIG. 4. Electric quadrupole frequency (ν_Q), asymmetry parameter (η) and site fractions (f) as a function of temperature obtained from the fit to experimental spectra for (a) sample 2 and (b) sample 3.

X-ray diffraction shows that samples of Gd_2O_3 crystallized in the cubic-C form of bixbiyte structure with space group $Ia3$. The unit cell of this structure contains 48 oxygen atoms and 32 Gd atoms occupying two nonequivalent sites: D sites, occupied by 8 Gd atoms with D_{3d} symmetry (axially symmetric), and C sites occupied by 24 Gd atoms with C_2 symmetry (highly asymmetric).[9] Therefore, it is expected that ^{111}Cd probe nuclei replace the two Gd sites. PAC spectra for samples 2 and 3 were fitted with a model of pure electric quadrupole interactions where probe nuclei occupy two site fractions. One of them with quadrupole frequency ν_{Q1} ~145 MHz and η = 0, which correspond to probe nuclei at sites D and another characterized by ν_{Q1} ~65 MHz and η ~0.95 (sample 2) and η ~0.85 (sample 3), which were ascribed to probe nuclei at sites C. These results are in good agreement with PAC results for commercial powder samples of Gd_2O_3 previously reported.[9] These results indicate that nanoparticles present a good crystallinity and although nanoparticles of sample 2 are small, with sizes around 10 nm, most part of them are in the expected crystalline structural for Gd_2O_3. PAC results for sample 1 were fitted with a broad frequency distribution compatible with very small nanoparticles. The hyperfine parameters obtained from the fits to experimental spectra

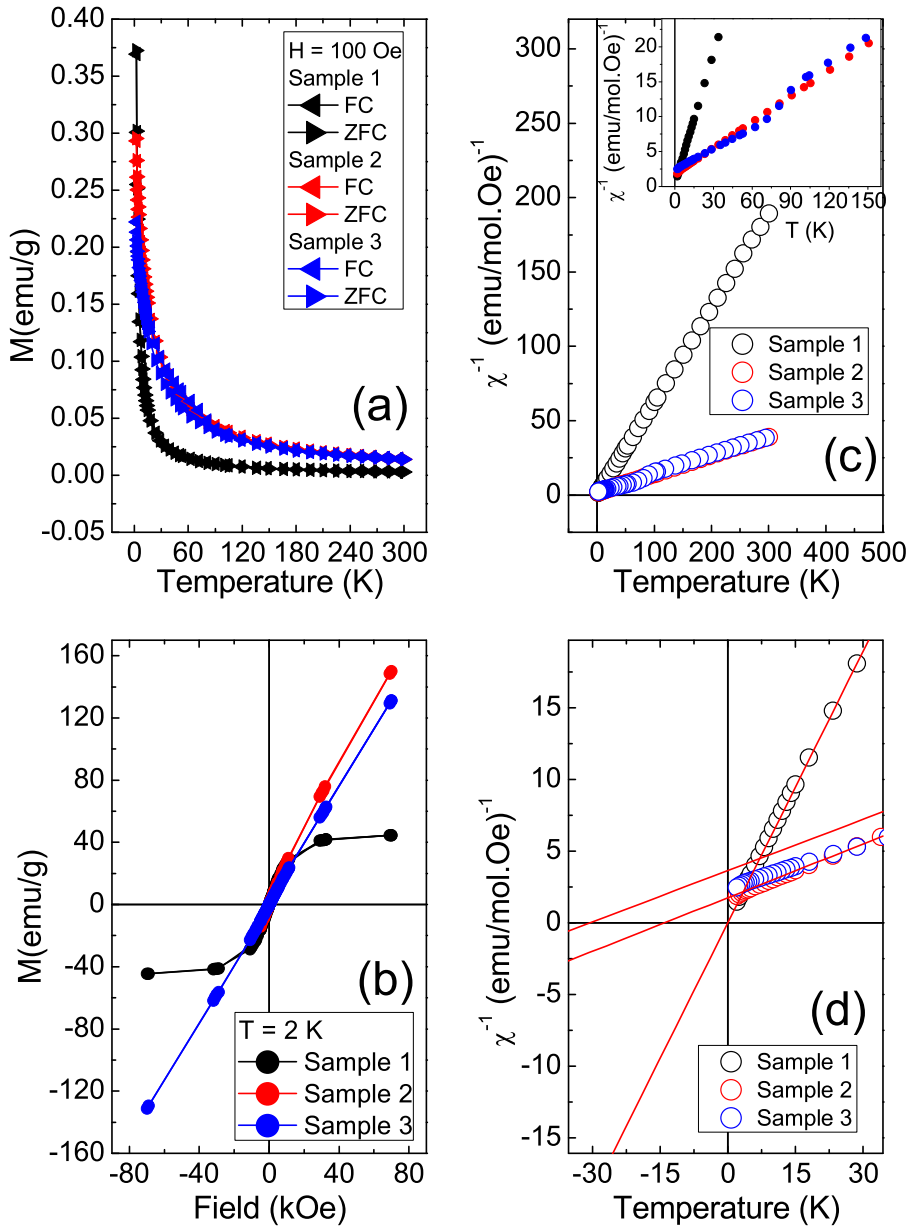

FIG. 5. (a) Zero-field-cooled (ZFC) and field-cooled (FC) dependence temperature under an applied field of 100 Oe. (b) Typical hysteresis curve under temperature of 2 K. (c) $1/\chi$ (where χ is the magnetic susceptibility) as a function of temperature. (d) Detailed $1/\chi$ showing an anti-ferromagnetic component for samples 2 and 3.

are displayed in Fig. 4. For two samples the quadrupole frequency and asymmetry parameters vary little with temperature and present almost the same behavior. The main difference is the temperature dependence of site fractions: fractions for sample 2 reach the expected proportion of site population (~75% for sites C and ~25% for sites D) around 700 K while fractions for sample 3 reach it around 450 K. This is a result of particle size which increases with the annealing temperature.

C. Magnetization

Magnetization as a function of temperature was obtained using zero-field-cooled (ZFC) and field-cooled (FC) procedure. In Fig. 5(a), the ZFC and FC curves present the same behavior with

TABLE I. Curie Constant (C), Curie-Weiss temperature (θ_{CW}) and effective moment (μ_{eff}) for samples 2 and 3.

Sample	C	θ_{CW} (K)	μ_{eff}
02	8.03	-14.1	8.01
03	8.40	-30.6	8.19

no indication of irreversibility temperature (T_{irr}) for all samples. The absence of a blocking temperature, usually associated with a maximum in the ZFC curve, suggest that the particles are not monodomain. Fig. 5(b) presents a typical hysteresis curve under temperature of 2 K. In Fig. 5(c) the inverse of the magnetic susceptibility as function of temperature is presented. The magnetic susceptibility follows the Curie-Weiss law $\chi = C/(T \pm \theta_{CW})$, where C is the Curie constant and θ_{CW} is the Curie-Weiss temperature. The Fig. 5(d) presents detailed portion of $1/\chi$ showing the presence of antiferromagnetic correlations in samples 2 and 3 and a paramagnetic behavior for sample 1. This difference in the magnetic behavior is probably due to the size of the particles, as sample 1 contains very small nanoparticles, the absence of crystallinity in these particles prevent the magnetic interaction between Gd ions. It is important to highlight that sample 1 magnetization values were normalized by mass for comparative purpose, since is not possible to know the amount of Gd in this sample. Results in table I presents C, θ_{CW} and effective moment (μ_{eff}) values for samples 2 and 3. Effective moment was calculated using $\mu_{eff} = 2.828(\mathrm{C})^{1/2}\mu_B$.

IV. SUMMARY

X-ray diffraction results showed that the samples crystallize in the cubic-C form has space group $Ia3$. Magnetization measurements showed an anti-ferromagnetic component for the samples 2 and 3 and paramagnetic behavior for sample1. Results show that sample annealed at 873 K present a quite good homogeneity and PAC results showed that the crystalinity of particles is preserve. In general, despite size changes, the magnetic and structural characteristics of Gd_2O_3 nanoparticles remain almost the same at different temperatures, showing that this compound is a good option for medical applications even under different conditions.

ACKNOWLEDGMENTS

Authors acknowledge to FAPESP and CNPq for partial financial support and to Dra. Rose Eli Rici (FMVZ - USP) and Me. Alfredo Duarte (IQ - USP) for TEM images.

[1] O. V. Salata, Journal of Nanobiotechnology **2**, 3 (2004).
[2] E. Boisselier, D. Astruc. Chem. Soc. Rev. **38**, 1759-1782 (2009).
[3] E. M. Pearce, J. B. Melanko, and A. K. Salem, Pharmaceutical Research **24**(12), 2335-2352 (2007).
[4] M. A. Albrecht, C. W. Evans, and C. L. Raston, Green Chem. **8**, 417-432 (2006).
[5] D. Kwatra, A. Venugopal, and S. Anant., Transl. Cancer Res. **2**(4), 330-342 (2013).
[6] J. Elias, Jr., A. C. Santos, M. Koenigkam-Santos, M. H. Nogueira-Barbosa, and V. F. Muglia, Radiol. Bras. **41**(4), 263-267 (2008).
[7] N. Sakai, L. Zhu, A. Kurokawa, H. Takeuchi, S. Yano, T. Yanoh, N. Wada, S. Taira, Y. Hosokai, A. Usui, Y. Machida, H. Saito, and Y. Ichiyanagi, Journal of Physics: Conference Series 352 (2012).
[8] C. Bouzigues, T. Gacoin, and A. Alexandrou, ACS Nano **5**, 8488-8505 (2011).
[9] J. Shitu, D. Wiarda, T. Wenzel, M. Uhrmacher, K. P. Lieb, S. Bedi, and A. Bartos, Phys. Rev. B. **46**, 7987-7993 (1992).
[10] E. L. Correa, B. Bosch-Santos, G. R. Veneziani, V. Vivolo, A. W. Carbonari, and M. P. A. Potiens, in Proceedings of the International Nuclear Atlantic Conference, São Paulo, SP, Brazil, October 4-9 (2015).
[11] B. Bosch-Santos, A. W. Carbonari, G. A. Cabrera-Pasca, and R. N. Saxena, Journal of Applied Physics **115**, 17E124 (2014), doi: 10.1063/1.4864439.
[12] A. W. Carbonari, R. N. Saxena, W. Pendl, Jr., J. Mestnik-Filho, R. N. Atilli, M. Olzon-Dionysio, and S. D. de Souza, J. Magn. Magn. Mater. **163**, 313-321 (1996).
[13] G. A. Cabrera-Pasca, A. W. Carbonari, B. Bosch-Santos, J. Mestnik-Filho, and R. N. Saxena, J. Phys.: Condens. Matter **24**, 416002 (2012).
[14] Z. Heiba, H. Okuyucuss, and Y. S. Hascicek, J. Appl. Crystallogr. **35**, 577-580 (2002).